3 Enzyme Kinetics of Drug-Metabolizing Reactions and Drug–Drug Interactions

MELISSA A. KRAMER
Bristol-Myers Squibb Company, Wallingford, CT, USA

TIMOTHY S. TRACY
Department of Experimental and Clinical Pharmacology, College of Pharmacy, University of Minnesota, Minneapolis, MN, USA

3.1 INTRODUCTION

In vitro studies play an important role in characterizing biotransformation reactions. Kinetic parameters are determined during the early phases of drug discovery and development and provide invaluable information needed to predict *in vivo* metabolism and assess potential interactions with enzyme effectors. These *in vitro* studies are routinely used for estimating kinetic parameters, such as K_m and V_{max}. Under linear conditions, the ratio of V_{max} and K_m represents the metabolic intrinsic clearance (CL_{int}), which is assumed to also be representative of the *in vivo* CL_{int} of a compound. Thus, it follows that this calculated CL_{int} value can then be used to extrapolate *in vitro* kinetic data to *in vivo* metabolic clearance and subsequently, the initial dose of a drug to be used in humans. To a great extent, this approach has provided reliable and successful *in vivo* clearance predictions. However, this success is predicated on accurate estimations of *in vitro* enzyme kinetic parameters. This chapter describes the proper conditions for carrying out *in vitro* enzyme kinetic experiments and the potential caveats that may lead to erroneous results. Also described are the various types of kinetic profiles that may be observed and equations that can be used to estimate kinetic parameters based

Encyclopedia of Drug Metabolism and Interactions, 6-Volume Set, First Edition.
Edited by Alexander V. Lyubimov.

on the type of kinetics. Finally, methods for determining a compound's potential for drug–drug interactions with other substrates of the same enzyme are described, along with kinetic models to assess inhibition potential.

3.2 CONFOUNDING FACTORS OF *IN VITRO* EXPERIMENTS

3.2.1 General *In Vitro* Incubation Conditions

It is vital to obtain reliable and accurate *in vitro* data that reflect the *in vivo* situation. Therefore, fundamentally sound enzyme kinetics practices must be employed and reaction conditions must be well defined. There are multiple factors to consider when determining which *in vitro* incubation conditions are appropriate and best mimic the *in vivo* system. The most important experimental components in drug metabolism reactions are substrate concentration, incubation time, and protein concentration. An appropriate length of time for an incubation reaction should allow for adequate product formation to ensure precise quantitation. It is equally important that the substrate turnover be linear with respect to incubation time and enzyme concentration. Initial experiments are needed, where product formation is measured at multiple time points in incubations containing different concentrations of protein. From these studies, an incubation time and protein amount can be chosen for all subsequent experiments where the same enzyme source is used. In practice, for many drug-metabolizing enzymes, a protein concentration of 0.1–0.25 mg/mL and an incubation time of 5–10 min will produce a linear reaction with readily detectable conversion of substrate (see below for discussion of the role of protein concentration and nonspecific binding to microsomal proteins). If nonlinearity is observed with respect to velocity, autoinactivation of the enzyme or too much substrate depletion may be occurring. The substrate concentration should be greater than 10-fold excess compared to the enzyme concentration, and $<10\%$ of the substrate should be consumed [1,2]. Experiments should include multiple time points (8–10 points), generally ranging from one-fifth to fivefold the K_m value. To this end, iterations of the experiment may be needed to establish the proper experimental conditions of enzyme concentration, time, and substrate concentration range to adequately describe the kinetic profile of the metabolism reaction.

Optimization of other experimental variables is equally as important when designing and conducting *in vitro* experiments to be used to determine kinetic parameters. Other important parameters that may affect metabolic rate and should be given careful consideration include selection of buffer system, buffer ionic strength, incubation pH, and incubation temperature. The *in vitro* experimental variables of temperature, pH, and buffer ionic strength are usually set to reflect human liver physiological conditions. Generally, one tries to employ buffer conditions that mimic the *in vivo* situation. For example, commonly used buffers include 50–100 mM potassium phosphate buffer or tris-hydroxyaminomethane (THAM) at pH 7.4 maintained at 37°C [3]. In addition, cosubstrates such as nicotinamide adenine dinucleotide phosphate (NADPH) or uridine diphosphate glucuronic acid (UDPGA) should not be rate limiting and are typically included at saturating concentrations during the incubation. Typical concentrations of NADPH used range from 0.5 to 2 mM and UDPGA, 3–5 mM. Alternatively, an NADPH-regenerating system may be utilized if one is concerned about maintaining NADPH concentrations, especially over longer incubation periods. However, typically

this is not an issue in incubations up to 1 h since the concentrations of NADPH suggested are significantly above the K_m for NADPH and, thus, depletion due to conversion to NADP is not usually an issue. Because the composition of the incubation matrix could potentially affect various enzymes differently, a systematic evaluation should be conducted to determine optimal experimental conditions [4,5].

Multiple studies have evaluated the effects of different buffering systems on kinetic parameter estimates; however, not all the reported findings are in agreement [6,7]. Irrespective of which buffer is chosen for the incubation mixture, it is important to maintain pH within the physiological range. Yao and Levy [3] have reported differences in *in vitro* K_i values due to small changes in pH from 7.2 to 7.6. These findings suggest that this should be an area of further research in order to optimally define *in vitro* incubation conditions that most accurately reflect the microenvironment of hepatic smooth endoplasmic reticulum.

3.2.2 Effect of Organic Solvents on Enzyme Activity

In an attempt to mimic the microenviroment of the human liver, *in vitro* studies are carried out in aqueous physiological buffers. However, owing to the lipophilic nature of many drug substrates and inhibitors, potential solubility problems arise. To overcome these issues, organic solvents such as methanol, ethanol, acetonitrile, and dimethyl sulfoxide (DMSO) are commonly used to facilitate compound solubilization. The presence of organic solvents in the incubation reaction may, however, alter enzyme–substrate interactions by modifying the native enzyme environment or altering enzyme activity. It is important that one considers these potential effects because any changes resulting from the presence of organic solvent could potentially compromise the reliability and interpretation of the *in vitro* data.

The effect of organic solvents in the incubation reaction on individual cytochrome P450 (CYP) enzyme activity of microsomal, hepatocyte, and recombinant enzyme systems has extensively been investigated [8–11]. The observed effect on individual CYP activity is solvent specific. For example, Vuppugalla *et al*. [10] reported no effect on CYP2B6 or CYP2C8 activity when 0.5% (v/v) methanol was present, whereas the presence of ethanol, acetonitrile, and DMSO showed concentration-dependent inhibition from 0.2% to 5%. Although results typically are in agreement, some discrepancies have been reported. It has been reported that 1% acetonitrile has no effect on CYP1A2 activity in human hepatocytes [11] or on cDNA-expressed recombinant enzymes [8], but it results in increased CYP1A2 activity in human liver microsomes [12,13]. These results suggest that the degree of inhibition may be enzyme-source dependent.

Although numerous studies have reported inhibitory effects on CYP enzyme activity because of the presence of organic solvent, stimulatory effects have been observed [8,14,15]. The presence of acetone (2–4% v/v) or acetonitrile (2–4% v/v) in kinetic studies using human liver microsomes or reconstituted CYP2C9 resulted in increased tolbutamide hydroxylation. The reported stimulatory effect was observed over a wide range of substrate concentrations. Similar findings were described by Tang and others [9] who observed an increase in CYP2C9 activity toward diclofenac 4′-hydroxylation and tolbutamide methyl hydroxylation. However, acetonitrile inhibited celecoxib methyl hydroxylation, suggesting that the stimulatory effect of acetonitrile on CYP2C9 activity is substrate dependent.

A given organic solvent may exhibit differential inhibitory or stimulatory effects on specific CYPs. Although purely aqueous incubation conditions are preferred for *in vitro* CYP metabolism studies, in practice, it is likely that the use of organic solvent will be required to facilitate enhanced solubility of the compound of interest. Thus, the organic solvent concentration must be kept to an absolute minimum and, generally, $<1\%$ of the total reaction volume. In addition, it is important to identify suitable solvents that enable *in vitro* studies to be completed with minimal effect on CYP activity.

3.2.3 Nonspecific Microsomal Binding

Human liver microsomes are the most popular and widely used *in vitro* system for evaluating drug metabolism due in part to their reasonable availability, low cost, and ease of use. However, numerous examples exist in the literature of nonspecific binding of drug substrates (and inhibitors) to microsomal proteins. Margolis and Obach [16] reported that the use of high microsomal protein concentrations (especially 0.5 mg/mL and greater) caused alterations of inhibition constants for drugs that were highly lipophilic because of nonspecific binding effects. Therefore, it is desirable to use the lowest amount of protein that yields quantifiable amounts of metabolite in order to minimize these effects [1,2]. Lipophilicity is a characteristic shared by most drugs, and therefore, it is not surprising that many substrates have been shown to readily bind nonspecifically to the protein milieu of the microsomal membrane. The extent of nonspecific binding varies among drug classes and is dictated by the physiochemical characteristics of the drug [17–19]. Drugs that are weak bases, such as amiodarone and amitriptyline, bind extensively to the microsomal membrane, whereas others that are weak acids, such as naproxen and tolbutamide, exhibit relatively little or no microsomal binding [18–20]. When drugs bind nonspecifically to microsomal proteins, the effective free substrate concentrations will be less than the amount added, leading to inaccuracies in the determination of K_m and K_i parameters. The apparent K_m (or K_i value in the case of inhibition experiments) observed will be higher than the true K_m, although there should be no effect on V_{max} [20]. Thus, an overestimation of K_m occurs and *in vivo* drug clearance will be underestimated, unless the actual free substrate concentration in the reaction mixture is determined (i.e., nonspecific binding is measured). Several groups have proposed various correction factors to be applied for nonspecific binding during extrapolation to *in vivo* clearance [19–21]. For drugs that exhibit extensive nonspecific binding, correction for microsomal binding using free fraction in incubation matrices improves the prediction of *in vivo* clearance values calculated from *in vitro* estimates of intrinsic clearance. However, one cannot simply correct the apparent K_m value by multiplying the unbound drug fraction because this rule does not apply to every enzymatic reaction [9].

3.3 DETERMINATION OF ENZYME KINETICS

3.3.1 Michaelis–Menten Kinetics

In typical enzyme-catalyzed reactions, the substrate and product concentrations are much greater than the enzyme concentration such that each enzyme molecule catalyzes the conversion of multiple substrate molecules to product. The conversion of substrate

to product involves the formation of a transition state that occurs at the catalytic, or active, site of the enzyme.

Generally, kinetic characterizations of most enzymatic reactions are governed by hyperbolic kinetics that can be described by the Michaelis–Menten equation (Eq. 3.1).

$$v = \frac{V_{\max}{}^{*}[\mathrm{S}]}{K_{\mathrm{m}} + [\mathrm{S}]} \tag{3.1}$$

The Michaelis–Menten equation is a quantitative description of the relationship that exists among the rate of an enzyme-catalyzed reaction (v), the concentration of substrate [S], and the two parameters, $V_{\max}$ and K_{m}. In this case, $V_{\max}$ is the maximal velocity of the reaction and K_{m} is the Michaelis constant. General characterization of the enzymatic reaction can be determined in terms of rate and concentration by means of this equation. However, it is important to keep in mind three general considerations that are made when describing kinetic data modeled after the Michaelis–Menten equation: (i) the enzymatic reaction is operating under steady-state conditions, (ii) rapid equilibrium between the concentration of all the enzyme–substrate intermediates becomes constant soon after initiation of the reaction, and (iii) the catalytic active site of the enzyme contains only one binding site at which one substrate molecule can interact at a given time.

The fundamental concepts underlying these kinetic analyses continue to provide the cornerstone for understanding drug metabolism today, and are routinely used during drug development to determine kinetic constants ($V_{\max}$ and K_{m}) in the analysis of *in vitro* drug metabolism data. The Michaelis constant, K_{m}, is strictly defined as the concentration of substrate at which half-maximal velocity of the reaction is achieved. It is important to recognize that the determination of this rate constant results from the combination of several rate constants such that K_{m} is equal to (Scheme 3.1), where E, S, ES, and P are the concentrations of the enzyme, substrate, substrate-bound enzyme, and enzyme products (metabolites), respectively. The association rate constant of $\mathrm{E} + \mathrm{S} \rightarrow \mathrm{ES}$ is depicted as k_1, whereas k_{-1} is the dissociation rate constant for $\mathrm{ES} \rightarrow \mathrm{E} + \mathrm{S}$ and k_2 is the dissociation rate constant of $\mathrm{ES} \rightarrow \mathrm{E} + \mathrm{P}$. Often, K_{m} is incorrectly associated with the affinity of the substrate for the enzyme, but as can be seen from the above discussion, K_{m} is a composite of three rate constants. More exactly, k_{-1}/k_1 (referred to as K_{s} or K_{d}), which is the substrate dissociation constant, reflects substrate affinity.

The definition of $V_{\max}$ is derived from the product of k_{cat} and e_0 ($k_{\mathrm{cat}} \times e_0$), where k_{cat} (or k_2, as referred to in Scheme 3.1) is the capacity of the enzyme–substrate complex to form product and e_0 is the enzyme concentration. The k_{cat} parameter is a reflection of the number of molecules of substrate that one molecule of enzyme can convert to product per unit time. For this reason, k_{cat} is also referred to as the *catalytic constant* or the *turnover number*.

The velocity of the reaction can be characterized as a hyperbolic, saturating profile. The key features of the substrate concentration versus reaction velocity plot are depicted

$$\mathrm{E} + \mathrm{S} \underset{k_{-1}}{\overset{k1}{\rightleftharpoons}} \mathrm{ES} \xrightarrow{k2} \mathrm{E} + \mathrm{P}$$

Scheme 3.1

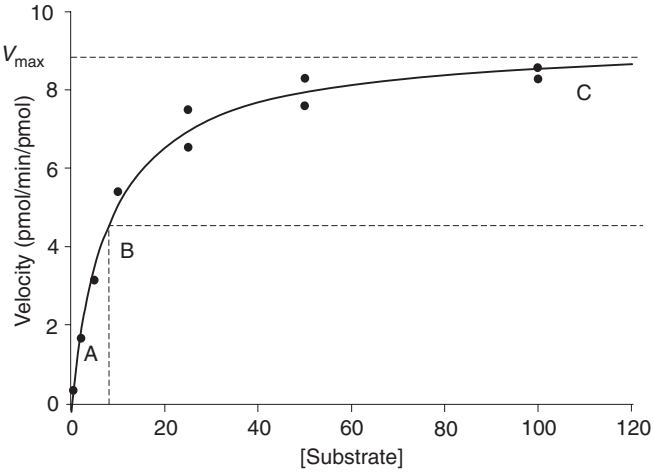

Figure 3.1 Hyperbolic saturation curve depicting typical Michaelis–Menten kinetics.

in Fig. 3.1. At high substrate concentrations, the rate of the reaction, represented by the point C, is almost equal to V_{max}, and rate differences at reasonably similar substrate concentrations are negligible. It should be noted that V_{max} is only an estimate, as the maximal velocity of the enzymatic reaction is never reached at a finite substrate concentration. If, however, the Michaelis–Menten plot is extrapolated to infinitely high substrate concentrations, the extrapolated rate is equal to V_{max}. At this point, the reaction becomes nearly independent of substrate concentration, and the rate is said to be zero order. At lower substrate concentrations, such as the areas of the curve before K_m (point B), the lower reaction velocities are indicative of only a portion of the enzyme molecules being occupied by substrate. Therefore, at low substrate concentrations (i.e., point A), the rate of the reaction is directly proportional to substrate concentration and the reaction is said to be first order.

Estimation of K_m and V_{max} is useful during the drug development process since these parameters can be used to estimate the *in vitro* intrinsic clearance (CL_{int}) for a drug, which in turn can be extrapolated to estimate the *in vivo* CL_{int}. The extrapolated parameter (CL_{int}) can then be used to predict *in vivo* hepatic clearance and subsequently total (systemic) clearance, and drug dosing. To do this, one makes the assumption that *in vivo*, the substrate concentration will be much lower than the K_m. Under these conditions, the [S] term drops out of the denominator and Equation 3.1 becomes Equation 3.2.

$$v = \frac{V_{max}[S]}{K_m} \tag{3.2}$$

In Equation 3.2, the velocity is proportional to [S] and is equal to the product of CL_{int} and [S] (Eq. 3.3).

$$v = CL_{int}[S] \tag{3.3}$$

Since *in vivo* CL_{int} is defined as the ability to clear drug in the absence of blood flow or protein-binding restrictions, the *in vivo* CL_{int} should be equal to the *in vitro*

CL_{int}. Because Equations 3.2 and 3.3 are analogous, the equations can be rearranged as (Eq. 3.4)

$$CL_{int} = \frac{V_{max}}{K_m} = \frac{v}{[S]} \tag{3.4}$$

This equation then allows derivation of CL_{int} following estimation of the *in vitro* enzyme parameters, K_m and V_{max}.

3.3.2 Non-Michaelis-Menten Kinetics

Unfortunately, not all enzyme reactions carried out by drug-metabolizing enzymes can be adequately described by Michaelis–Menten kinetics (i.e., they do not exhibit a hyperbolic kinetic profile). These types of kinetic profiles have been observed with several of the CYP drug-metabolizing enzymes, most commonly, CYP3A4, and also with most other drug-metabolizing CYPs. However, atypical kinetic profiles have also been observed with other important drug-metabolizing enzymes such as the UGTs (UDP-glucuronosyltransferases) [22–24].

Most commonly, atypical kinetic profiles observed with drug-metabolizing enzymes have been attributed to the binding of multiple molecules of a substrate (homotropic) or two chemically different substrate molecules (heterotropic) within the enzyme active site. The binding of one molecule can change the kinetics of a second substrate molecule binding within the active site and is frequently referred to as *cooperativity*. This cooperativity is characterized as being homotropic or heterotropic depending on the chemical species present in the enzyme active site. This cooperativity can be either positive or negative, depending on the effects elicited by the second substrate molecule. Although the term *allosterism* is generally used to describe cases where a second molecule binding distant to the substrate molecule causes an alteration in the functioning of the enzyme, it is also sometimes used to describe the kinetic changes due to a second substrate molecule binding since it is separate from the original substrate but may be still within the active site. However, it should also be realized that these types of kinetics may also be due to the presence of multiple species of the enzyme (e.g., conformers) that exhibit different kinetic characteristics with a substrate.

3.3.2.1 Sigmoidal Kinetics. Numerous examples of activation, or positive cooperativity, in drug-metabolizing enzymes are found throughout the literature [25]. Activation occurs when enzyme activity for a substrate is increased either by the presence of another compound or a single compound activating its own metabolism. Autoactivation is an example of homotropic cooperativity and is characterized by a sigmoidal kinetic profile. This profile is thought to occur because of the simultaneous binding of two molecules of the substrate within the enzyme active site, with the metabolism of one of the substrate molecules exhibiting a low K_m and low V_{max} and the other exhibiting a higher K_m and higher V_{max} (Fig. 3.2). A useful tool in establishing the presence of sigmoidicity in a kinetic plot is to identify deviations from linearity when the data are presented in an Eadie–Hofstee plot. A marked increase in the curvature, or hooked nature, of the line is indicative of a sigmoidal profile (Fig. 3.3). These data are indicative of positive cooperativity and suggest the presence of multiple interactions between the substrate and enzyme. Altered affinity and rate of product formation for other substrate binding sites may result from these interactions.

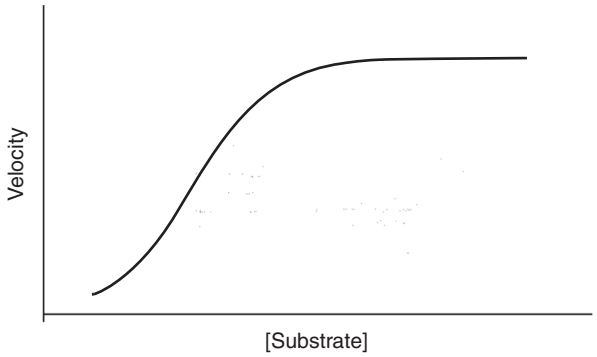

Figure 3.2 Sigmoidal saturation curve of velocity versus substrate concentration.

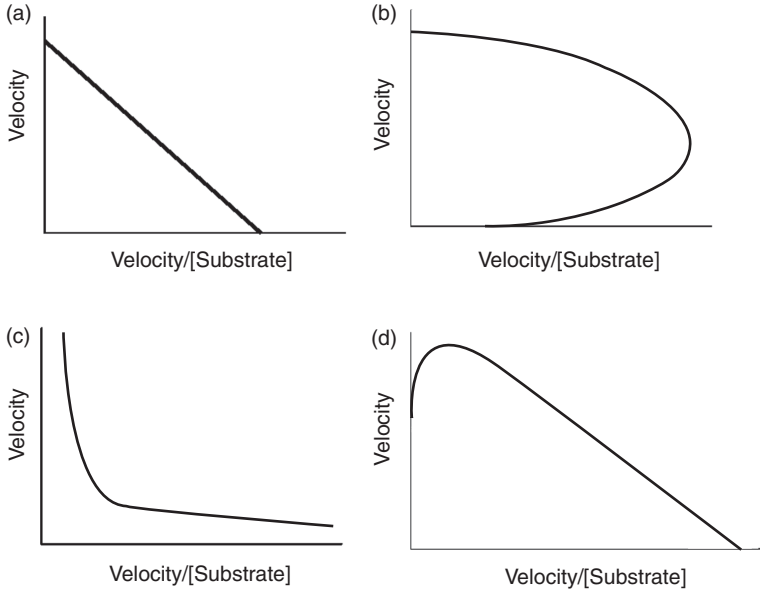

Figure 3.3 Eadie–Hofstee plots of typical and atypical kinetics. (a) Hyperbolic (Michaelis–Menten kinetics), (b) sigmoidal kinetics, (c) biphasic kinetics, and (d) substrate inhibition kinetics.

One of the most commonly used equations to describe sigmoidal kinetic profiles is the Hill equation [26] and is commonly used to mathematically describe sigmoidal kinetic profiles (Eq. 3.5).

$$v = \frac{V_{\max}[\mathrm{S}]^n}{K' + [\mathrm{S}]^n} \tag{3.5}$$

Although the K' parameter is analogous to K_{m}, it is not equivalent (unless $n = 1$) as it is composed of both K_{m} and the interaction factors [27]. The coefficient n, referred to as the *Hill coefficient*, reflects the degree of cooperativity observed. It should be

noted that n does not relate to the number of binding sites within the enzyme. Values of $n > 1$ are indicative of positive cooperativity, and the greater the n value, the greater the sigmoidicity of the kinetic profile.

Although applicable to most sigmoidal kinetic data, the Hill equation provides limited information about the actual kinetic processes and the associated rate constants. In an attempt to overcome these limitations and gain additional insight into the substrate–enzyme interaction, more complex kinetic models have been proposed [28,29]. These models are based on the assumption of two equivalent substrate binding sites within the enzyme active site. Korzekwa *et al*. [29] derived velocity equations to fit sigmoidal kinetic observations, thereby allowing one to estimate two K_m values (K_{m1} and K_{m2}) and two V_{max} values ($V_{max\,1}$ and $V_{max\,2}$) (Eq. 3.6), ostensibly representing the kinetic processes at each of the binding sites.

$$v = \frac{\frac{V_{max\,1}}{K_{m1}} + \frac{V_{max\,2}}{K_{m1}K_{m2}}}{1 + \frac{[S]}{K_{m1}} + \frac{[S]^2}{K_{m1}K_{m2}}} \tag{3.6}$$

A more detailed model that provided additional insights into the micro rate constants of the various processes was proposed by Shou *et al*. [27], again modeling two binding sites within the enzyme active site. A kinetic scheme was proposed that discriminates all possible equilibrium and rate steps of each of the enzyme–substrate complexes possible within the two binding sites.

The following equation (Eq. 3.7) was derived based on Scheme 3.2 for estimation of the associated kinetic parameters:

$$\frac{v}{[E]_{total}} = \frac{\frac{k_\alpha}{K_{S1}} + \frac{k_\beta}{K_{S2}} + \frac{[S]}{K_{S1}\times K_{S3}} \times (k_\delta + k_\gamma)}{\frac{1}{[S]} + \frac{1}{K_{S1}} + \frac{1}{K_{S2}} + \frac{[S]}{K_{S2}\times K_{S4}}} \tag{3.7}$$

3.3.2.2 Biphasic Kinetics. Biphasic kinetic profiles are another example of homotropic cooperativity, but unlike sigmoidal kinetics, biphasic kinetics profiles do not reach saturation, but rather exhibit two distinct phases (Fig. 3.4). The first phase is observed at low substrate concentrations and is more characteristic of hyperbolic

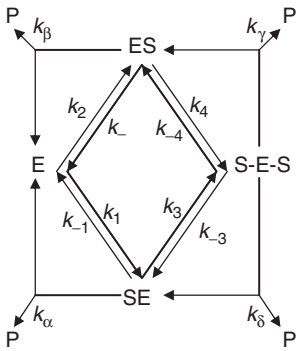

Scheme 3.2

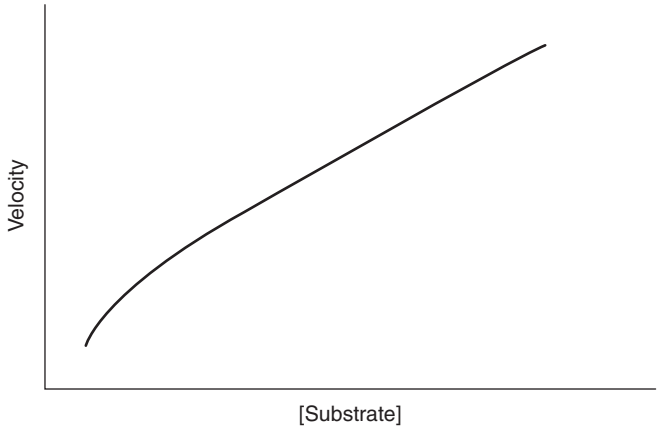

Figure 3.4 Biphasic saturation curve of velocity versus substrate concentration.

kinetics. At increasing substrate concentrations, the second phase becomes evident as the velocity of the reaction continues to increase linearly, with no evidence of saturation. However, one must be cognizant that "apparent" biphasic kinetic profiles may appear in multienzyme systems, where two enzymes are producing the same metabolite but with dramatically different kinetics, such that one enzyme is a high affinity–low capacity enzyme and the second enzyme is a low affinity–high capacity enzyme. In true biphasic kinetics, the same enzyme is operating with both a low- and high-affinity binding component [29]. If a biphasic kinetic profile is observed within a single enzyme system, it most likely results from multiple binding regions within the active site, or the substrate binds within the active site in multiple orientations. Regardless, the binding orientation responsible for the semihyperbolic portion of the profile will result in a low K_m, low V_{max} component, whereas the other binding orientation will produce a high K_m and high V_{max}. A kinetic equation has been developed, essentially a combination of the Michaelis–Menten equation and a linear equation, to describe biphasic kinetics (Eq. 3.8):

$$v = \frac{(V_{max\,1}[S]) + (CL_{int}) \times [S]^2}{(K_{m1} + [S])} \tag{3.8}$$

From this equation, the parameters derived from fitting the equation to the initial curved portion of the plot provide estimates of $V_{max\,1}$ and K_{m1} and are reflective of low substrate concentrations. The CL_{int} parameter describes the linear portion of the profile that occurs at high concentrations and can be determined from the ratio of $V_{max\,2}/K_{m2}$ (i.e., the slope of the linear portion of the kinetic profile).

3.3.2.3 Substrate Inhibition. Substrate inhibition occurs when the rate of product formation plateaus at a point and then decreases with increasing substrate concentrations (Fig. 3.5). To model substrate inhibition and derive kinetic parameter estimates, an equation has been derived based on the uncompetitive inhibition model (Eq. 3.9). From this equation, one can estimate the kinetic parameters K_m, V_{max}, and K_{si} (i.e., inhibition constant for the second substrate molecule).

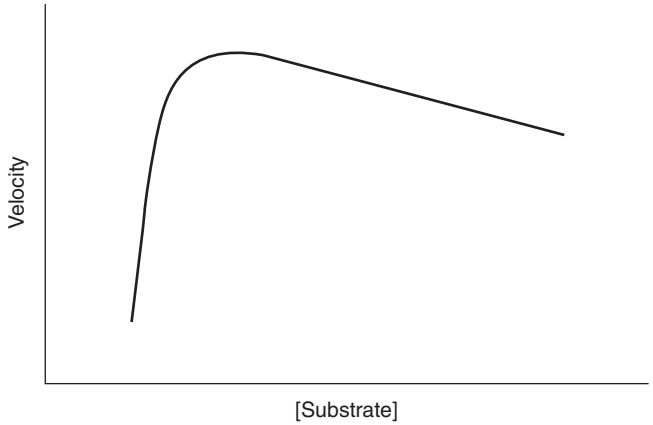

Figure 3.5 Substrate inhibition saturation curve of velocity versus substrate concentration.

$$v = \frac{V_{\max}[\mathrm{S}]}{K_{\mathrm{m}} + [\mathrm{S}] + \frac{[\mathrm{S}]^2}{K_{\mathrm{si}}}} \tag{3.9}$$

However, this kinetic model, apart from the K_{m} and $V_{\max}$ estimations, only provides insight into the inhibition constant of the substrate and not into more of the micro rate constants of formation and dissociation of the various possible species present. To better describe the various rate constants associated with all possible species and processes involved in substrate inhibition, a more complex kinetic model was proposed (Scheme 3.3) [30].

This model is based on the premise that one binding site is catalytic and the other inhibitory and that substrate molecules have access to both these sites. When the substrate (S) binds to the catalytic site of the enzyme (i.e., ES), the rate and $V_{\max}$ of product formation (ES $\rightarrow$ P) are determined by $k_{\mathrm{p}}[\mathrm{ES}]$ and $k_{\mathrm{p}}[\mathrm{E}]_{\mathrm{total}}$, respectively. In contrast, once excess S binds to the nonproductive, inhibitory site (SE) the rate of S-E-S is no longer the same as ES and is reduced by a factor β. This model incorporates sequential binding of substrate molecules such that the substrate inhibition site cannot

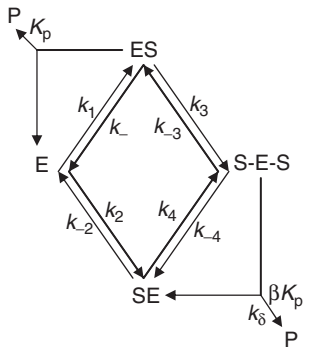

Scheme 3.3

be occupied until the active site is filled and the second site may be independent from the active site.

On the basis of this scheme, an equation was derived to describe substrate inhibition, based on the assumption that the rates of formation and of decomposition of the various enzyme–substrate complexes are equivalent (Eq. 3.10) [30].

$$v = \frac{V_{\max}\left[\frac{1}{K_S} + \frac{\beta \times [S]}{(\alpha \times K_i \times K_S)}\right]}{\frac{1}{S} + \frac{1}{K_S} + \frac{1}{K_i} + \frac{[S]}{(\alpha \times K_S \times K_i)}} \tag{3.10}$$

In this equation, K_S is approximately equal to K_m, and K_i is the dissociation constant of the substrate binding to the inhibitory site. Alpha (α) represents the factor by which the dissociation of substrate (K_S and K_i) at both sites is altered when a second molecule is bound, whereas β is the factor by which V_{max} changes on binding of a second substrate molecule. It is evident that the use of this equation allows for additional parameter estimations and provides useful information as to the degree to which binding of the second substrate molecule alters K_m and V_{max}. However, it should be noted that because of the number of parameters to be estimated, properly fitting data to this equation requires acquisition of a substantial number of data points.

3.3.2.4 Heteroactivation Kinetics. During *in vitro* studies to evaluate potential drug–drug interactions, one typically expects to observe inhibition using microsomal or expressed enzyme systems. However, it is now well established that *in vitro* coincubation of two different compounds can also result in increased metabolism of one substrate rather than inhibition [25,29] (Fig. 3.6). Again, this phenomenon

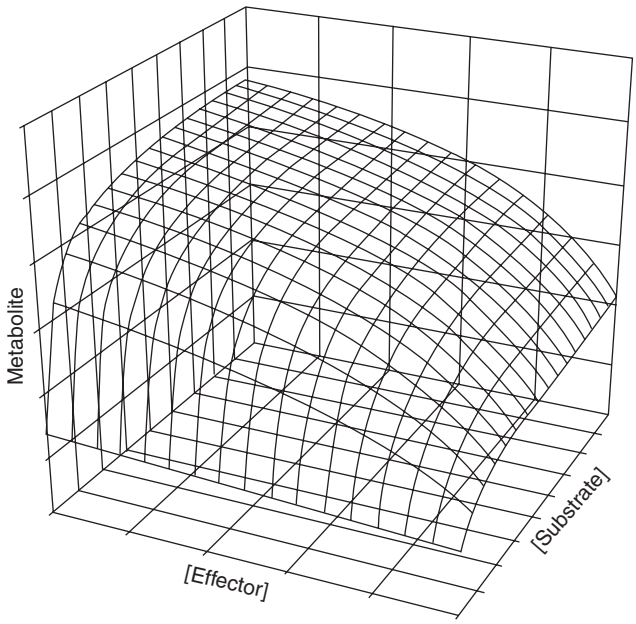

Figure 3.6 Heteroactivation plot depicting the relationship between the metabolite, effector molecule, and substrate.

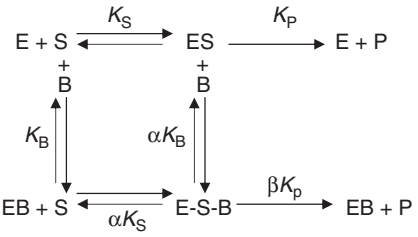

Scheme 3.4

has been attributed to the simultaneous binding of two different molecules, substrate and effector, within the active site. However, it should be realized that the "effector" may also be metabolized itself. This positive cooperativity typically results in both a decrease in K_m and an increase in V_{max}. This heteroactivation is depicted in Scheme 3.4.

This kinetic scheme has been described by a complex equation (Eq. 3.11) that allows for determination of the kinetic parameters above:

$$v = \frac{V_{max} \times [S]}{K_m \left(\frac{1+\frac{[B]}{K_B}}{1+\frac{\beta[B]}{\alpha K_B}} \right) + [S] \left(\frac{1+\frac{[B]}{\alpha K_B}}{1+\frac{\beta[B]}{\alpha K_B}} \right)} \tag{3.11}$$

where B is the concentration of activator, α is the factor by which the K_m for substrate changes, and β can be thought of as the factor by which V_{max} changes. This equation allows for fitting multiple curves representing different activator concentrations and has a manageable number of parameters including the usual K_m and V_{max} for substrate in the absence of activator.

3.4 GRAPHICAL PRESENTATION OF KINETIC DATA TO IDENTIFY ATYPICAL KINETIC PHENOMENA

The most appropriate method of generating enzyme kinetic parameter estimates is the use of computer-generated, nonlinear regression analysis of the untransformed data using a suitable model. However, in the analysis of enzyme kinetics data, much value can be gained by examining a graphical representation of the kinetic data. Graphical plotting of the data can provide additional insights into interpretation of whether the data are truly hyperbolic and follow Michaelis–Menten kinetics or whether atypical kinetic phenomena may be operational. Thus, graphical presentations of the data can aid in determining the correct kinetic model to apply in estimating kinetic parameters.

3.4.1 Eadie–Hofstee Plot

The Eadie–Hofstee plot is based on the transformation of the Michaelis–Menten equation to give the equation of a straight line. In this case, the v is plotted along the y-axis and v/[S] along the x-axis (Fig. 3.3). The slope of the best-fit line is equal to $-K_m$, the y-intercept $= V_{max}$, and the x-intercept $= V_{max}/K_m$. As with other graphical

representations, the Eadie–Hofstee plot is not without caveats. The Eadie–Hofstee plot has the disadvantage that the velocity appears in both coordinates. Because the x-axis contains an element of the velocity, it no longer reflects a truly independent variable. As a result, any experimental errors will be reflected on both axes. Therefore, otherwise seemingly good data can appear worse. On the other hand, this plot best reveals the presence of atypical kinetic profiles based on the shape of the data-fit obtained. For example, a linear Eadie–Hofstee plot of the data would be representative of hyperbolic (Michaelis–Menten) kinetics, a "hooked" Eadie–Hofstee plot suggests sigmoidal autoactivation kinetics, a biphasic Eadie–Hofstee plot suggests biphasic kinetics, and an Eadie–Hofstee plot where the plot rises and then falls similar to the substrate versus velocity plot of substrate inhibition would, of course, suggest that substrate inhibition is occurring.

3.5 DRUG–DRUG INTERACTIONS DUE TO ENZYME INHIBITION

Drug–drug interactions continue to be an obstacle for the pharmaceutical industry, and thus, accurate predictions of potentially adverse clinical outcomes become increasingly important in drug discovery and development. The determination of *in vitro* enzyme inhibition kinetics is an important predictor of potential drug–drug interactions. Enzyme inhibition is the decrease in the rate of substrate turnover in the presence of an inhibitory effector molecule. Enzyme inhibitors fall into two broad classes—reversible and irreversible [30]. Reversible inhibitors bind to enzymes through weak, noncovalent interactions such as hydrogen bonds, hydrophobic interactions, and ionic bonds. The sum of the multiple weak interactions between the inhibitor and the enzyme active site results in strong, specific but still reversible binding [31]. In contrast, irreversible, or mechanism-based, inhibitors cause enzyme inactivation through covalent or quasi-irreversible modification of the enzyme structure. The following sections discuss both classes of inhibition, as well as the meaning of the inhibition kinetic parameters, IC_{50} and K_i.

3.5.1 Reversible Inhibition

3.5.1.1 Competitive Inhibition. The simplest and most commonly observed type of reversible enzyme inhibition is that of competitive inhibition. As the name implies, a substrate and inhibitor are competing for the enzyme active site, and their binding is mutually exclusive. The inhibitor may bind to the same binding region of the substrate or partly mask it. In either case, when the inhibitor is bound to the enzyme, the substrate is unable to bind in a productive orientation and the complex is incapable of catalysis of substrate. Competitive inhibition can be overcome by sufficiently high concentrations of substrate. The kinetic scheme for this type of inhibition is shown in Scheme 3.5.

In case of competitive inhibition, there is no change in V_{max}; however, an increase in K_m is observed. When comparing inhibition potential of several compounds, it often helps to characterize the inhibition in terms of CL_{int}. Therefore, one can characterize competitive inhibition as resulting in a decrease in CL_{int} (V_{max}/K_m), with no change in the apparent V_{max}. The equation for competitive inhibition is shown in Equation 3.12.

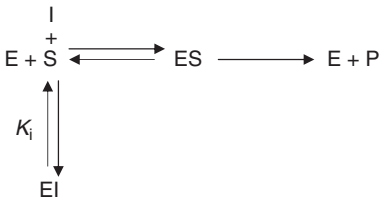

Scheme 3.5

$$v = \frac{V_{max} \times [S]}{K_m\left(1 + \frac{[I]}{K_i}\right) + [S]} \tag{3.12}$$

In this equation, V_{max} and K_m have their usual meanings and [I] is the free inhibitor concentration. K_i is the inhibition constant, and $K_i = [E][I]/[E]$, which when substituted into Equation 3.12, is in the same form as the Michaelis–Menten equation. From Equation 3.12, it becomes apparent that in the case of competitive inhibition, K_m is increased by a factor $(1 + [I]/K_i)$ and V_{max} remains unchanged.

3.5.1.2 Noncompetitive Inhibition. Purely noncompetitive inhibition is rarely observed in enzyme kinetics studies, except in the case of very small inhibitors (e.g., protons, metal ions, and small amides), but is included here for completeness. Noncompetitive inhibition is a form of mixed inhibition where the substrate and inhibitor bind reversibly and independently. In this case, the binding of the inhibitor to the enzyme reduces its activity but has no effect on the binding of the substrate. The kinetic scheme for noncompetitive inhibition is shown in Scheme 3.6.

An example of noncompetitive inhibition would be when the inhibitor binds to the enzyme somewhere other than the active site, thereby changing the enzyme's three-dimensional structure such that the active site is still able to bind substrate but is no longer in the optimal configuration to stabilize the transition state and catalyze the reaction. This type of inhibition results in a decrease in V_{max} and no apparent change in K_m. On closer examination, most situations originally thought to involve noncompetitive inhibition were actually cases of mixed inhibition. The equation for noncompetitive inhibition is shown below (Eq. 3.13).

$$v = \frac{V_{max}[S]}{K_m\left(1 + \frac{[I]}{K_i}\right) + [S]\left(1 + \frac{[I]}{K_i}\right)} \tag{3.13}$$

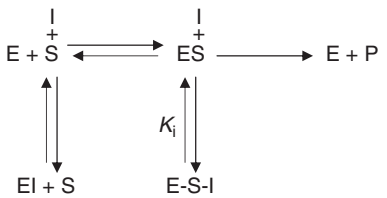

Scheme 3.6

3.5.1.3 Uncompetitive Inhibition. Uncompetitive inhibition occurs when an enzyme–inhibitor reversibly binds only to the enzyme–substrate (E–S) complex yielding an inactive enzyme-substrate-inhibitor (E-S-I) complex; the inhibitor does not bind to the free enzyme. However, uncompetitive inhibition is also not common. The kinetic model for this type of inhibition is shown in Scheme 3.7.

In this case, the reduction in the effective concentration of the ES complex results in a decreased K_m value and proportional decrease in V_{max}. As a result, the inhibitor has no net effect on V_{max}/K_m (i.e., enzyme efficiency or CL_{int}). The equation to describe uncompetitive inhibition constants, as well as values for K_m and V_{max}, is presented below (Eq. 3.14).

$$v = \frac{\left[\frac{V_{max}}{1+\frac{[I]}{K_i}}\right] + [S]}{\left[\frac{K_m}{1+\frac{[I]}{K_i}}\right] + [S]} \tag{3.14}$$

3.5.1.4 Mixed Inhibition. The effects of mixed inhibition on enzyme reactions are such that both specific and catalytic effects are present. As a result, this type of inhibition is characterized by a decrease in the maximal velocity (V_{max}) and an increase in the concentration at which half-maximal velocity (K_m) is achieved. This type of inhibition can be reduced, but not completely overcome, by increasing concentrations of substrate. The kinetic scheme for mixed inhibition is shown in Scheme 3.8, where K_i and K_i' represent the competitive and uncompetitive inhibition components, respectively.

From the kinetic scheme, it is clear that the mechanism that results in mixed inhibition is much more complex than that of others. In mixed inhibition, the substrate can bind to the enzyme–inhibitor complex, which can subsequently dissociate to form an enzyme–substrate complex capable of undergoing catalysis to produce product.

There are multiple binding mechanisms that may account for the observed effects on V_{max} and K_m in the presence of the inhibitor. First, the inhibitor can compete with

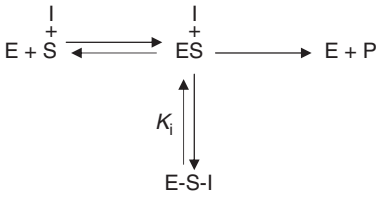

Scheme 3.7

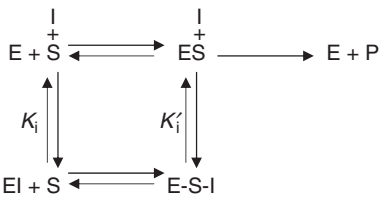

Scheme 3.8

the substrate for binding to the enzyme. Second, the inhibitor may bind to an enzyme molecule that subsequently binds to the substrate. Third, the inhibitor can bind to an enzyme–substrate complex and affect catalytic turnover. The effects of the mixed inhibition on the velocity of the reaction can be described by the following equation (Eq. 3.15).

$$v = \frac{V_{\max} \times [\mathrm{S}]}{K_{\mathrm{m}}\left(1 + \frac{[\mathrm{I}]}{K_{\mathrm{i}}}\right) + [\mathrm{S}]\left(1 + \frac{[\mathrm{I}]}{K_{\mathrm{i}}}\right)} \tag{3.15}$$

3.5.2 Irreversible Inhibition

3.5.2.1 Mechanism-Based Inhibition. Unlike reversible inhibition that involves rapid association and dissociation of drugs and enzymes, time-dependent inhibition involves irreversible covalent binding or quasi-irreversible tight binding of a chemically reactive intermediate to the heme of the CYP or to the protein itself [32]. In general, a time-dependent inhibitor is defined as a compound that exhibits increased inhibition when incubated with the enzyme before the addition of the substrate. Therefore, mechanism-based inhibitors qualify as a subset of time-dependent inhibitors, in which experimental evidence supports the formation of a chemically reactive metabolite capable of inactivating the enzyme [33].

The *in vitro* characterization of a mechanism-based inhibitor must satisfy seven criteria (see below) and includes the determination of three key parameters: the maximum inactivation rate constant (k_{inact}), the inactivator concentration that produces half-maximal rate of inactivation (K_{I}), and the efficiency of inactivation relative to metabolism, or partition ratio (r). The necessary criteria defining mechanism-based inhibition include (i) time dependence, (ii) saturation, (iii) substrate protection, (iv) irreversibility, (v) stoichiometry of inactivation, (vi) involvement of a catalytic step, and (vii) inactivation occurring before release of the activated species [34]. The kinetic scheme for mechanism-based inhibition is depicted below (Scheme 3.9), where EI* is the reactive form of EI, P is the metabolite product, and $\mathrm{E_i}$ is the inactivated enzyme. From the model, it is apparent that the enzyme kinetics involving mechanism-based inhibition are complex and are governed by the first-order rate constants k_1, k_{-1}, k_2, k_3, and k_4 [35].

A rate equation representing the loss of functional enzyme with time was described by Kitz and Wilson [36] (Eq. 3.16).

$$\frac{\mathrm{d}[\mathrm{E}]_t}{\mathrm{d}t} = \left(\frac{k_{\mathrm{inact}}[\mathrm{I}]}{K_{\mathrm{I}} + [\mathrm{I}]}\right)[\mathrm{E}]_t \tag{3.16}$$

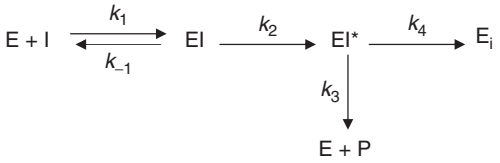

Scheme 3.9

$[E]_t$ represents the active enzyme concentration at time t; [I], the inactivator concentration; k_{inact}, the maximum inactivation rate constant; and K_I, the inactivator concentration that produces half-maximal rate of inactivation. From Equation 3.16, it is evident that the rate of P450 enzyme inactivation is proportional to the inactivator concentration and can be saturated at high concentrations [37]. Both k_{inact} and K_I are derived from complex relationships between the first-order rate constants (Eqs. 3.17 and 3.18, respectively).

$$k_{inact} = \frac{k_2 k_4}{k_2 + k_3 + k_4} \tag{3.17}$$

$$K_I = \left[\frac{k_{-1} + k_2}{k_1}\right]\left[\frac{k_3 + k_4}{k_2 + k_3 + k_4}\right] \tag{3.18}$$

The effects of a mechanism-based inhibitor on the velocity of the reaction can be described by Equation 3.19, where k_{cat} is defined by Equation 3.20.

$$v = \frac{k_{cat}[E]_t[I]}{K_m + [I]} \tag{3.19}$$

$$k_{cat} = \frac{k_2 k_3}{k_2 + k_3 + k_4} \tag{3.20}$$

The ratio of the metabolite formation rate to the inactive enzyme formation rate is referred to as the *partition ratio* (r) and is described in Equation 3.21.

$$r = \frac{k_{cat}}{k_{inact}} = \frac{k_3}{k_4} \tag{3.21}$$

The partition ratio can be used as a measure of efficiency of the mechanism-based inactivation process, thereby providing useful information regarding the inactivation potential of compounds in early drug discovery.

Experimental conditions employed to determine the kinetics of mechanism-based enzyme inactivation involve evaluation of the time dependence of the reaction. In these experiments, a preincubation (primary incubation) for specific time periods is conducted in the presence/absence of increasing concentrations of the putative inactivator and NADPH, followed by CYP activity measurement by dilution into a secondary incubation [38]. Typical results are depicted in Figs. 3.7 and 3.8.

The half-lives for inactivation of probe substrate at each concentration of inactivator can be calculated from the slopes of the individual lines to give k_{obs}, the pseudo first-order rate constant of inactivation at inactivator concentration [I] (Fig. 3.9). A double reciprocal plot of $1/k_{obs}$ versus 1/[I], known as *Kitz–Wilson plot*, can be constructed to obtain the inactivation parameters k_{inact} and K_I (Fig. 3.9) [36]. In the case of a saturation reaction, the concentration of the inactivator is infinite and there is a finite half-life, and the point where the plotted line intersects the y-axis is equal to $0.693/k_{inact}$. However, with commercially available graphing software, the inactivation parameters also can be determined by a direct plot of k_{obs} versus inactivator concentration followed by non-least-squares fitting [37].

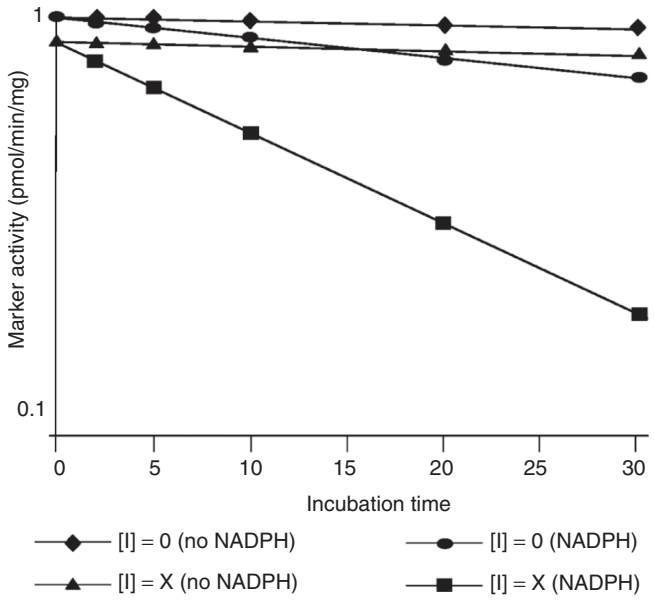

Figure 3.7 Evaluation of the time dependence of a mechanism-based inactivator in the presence/absence of NADPH.

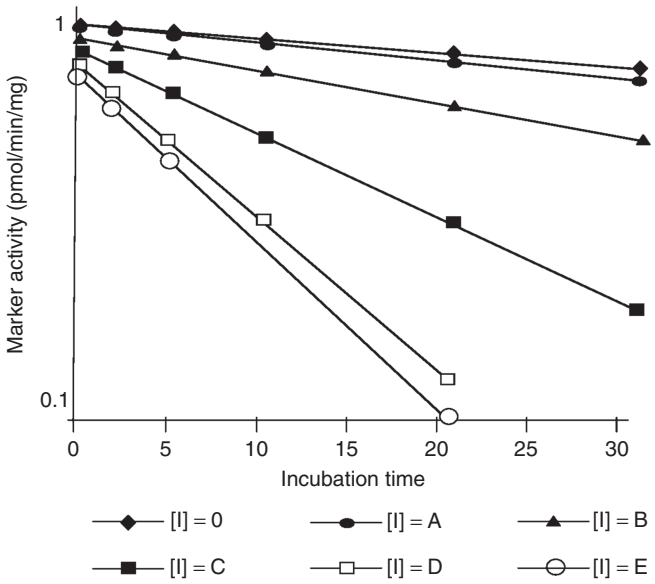

Figure 3.8 Evaluation of the time dependence of a mechanism-based inactivator in increasing concentrations of a putative inactivator.

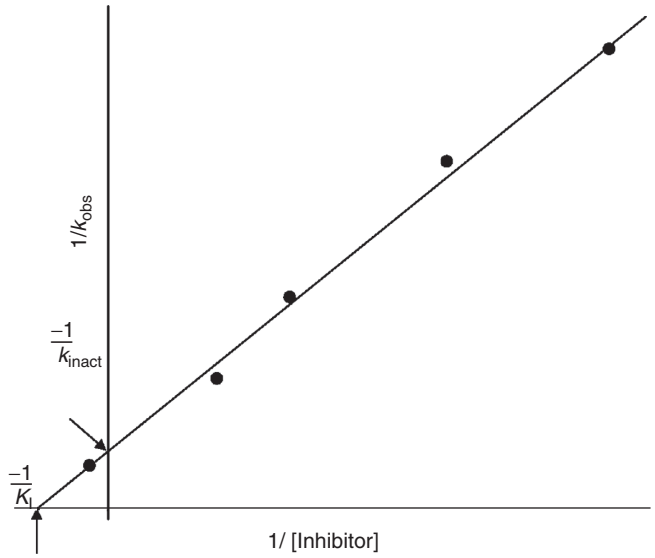

Figure 3.9 Kitz–Wilson double reciprocal plot depicting the relationship between k_{inact} and K_I.

3.5.3 Context of IC_{50} and K_i Parameters

The parameters of IC_{50} and K_i are used to describe the inhibitory potential of a compound and are routinely determined in early drug discovery to assess the potential inhibition liabilities for new molecular entities. Estimation of K_i follows the same guidelines as for estimating K_m; multiple substrate concentrations (usually three to four) and multiple inhibitor concentrations (usually four to five) should be used. The range of inhibitor concentrations also should be at least threefold above and below the estimated K_i value [39]. An appropriate definition or specification of the type of enzyme inhibition (e.g., competitive, noncompetitive, mixed) must be selected in order to determine an accurate estimation of K_i. Guidelines for the selection of a proper model have been previously described [37]. However, alternative methods for selecting an inhibition model have been reported [40].

Velocity equations for K_i determinations result in a 3D plot because of the presence of two variable parameters, substrate [S] and inhibitor [I] concentration. Linear transformation of the data, in the form of an Eadie–Hofstee plot (v vs [I]) or as a Dixon plot ($1/v$ vs [I]), allows for easier visualization of the data. The K_i value cannot be determined solely from these graphical representations; however, they are helpful in providing insight into possible inhibition mechanisms involved. In the Dixon plot, for example, if the lines intersect above the x-axis, it suggests competitive inhibition, whereas if the intersection is on the x-axis, it suggests mixed inhibition (Fig. 3.10). To avoid inaccuracies, K_i should always be determined by simultaneous nonlinear regression of the entire untransformed data set using a suitable software program.

In comparison to the K_i value, which represents the dissociation constant of the enzyme–inhibitor complex, an IC_{50} is simply defined as the inhibitor concentration that decreases the biotransformation of a substrate at a single, specified concentration by 50%. The two inhibition parameters cannot be used interchangeably. The IC_{50}

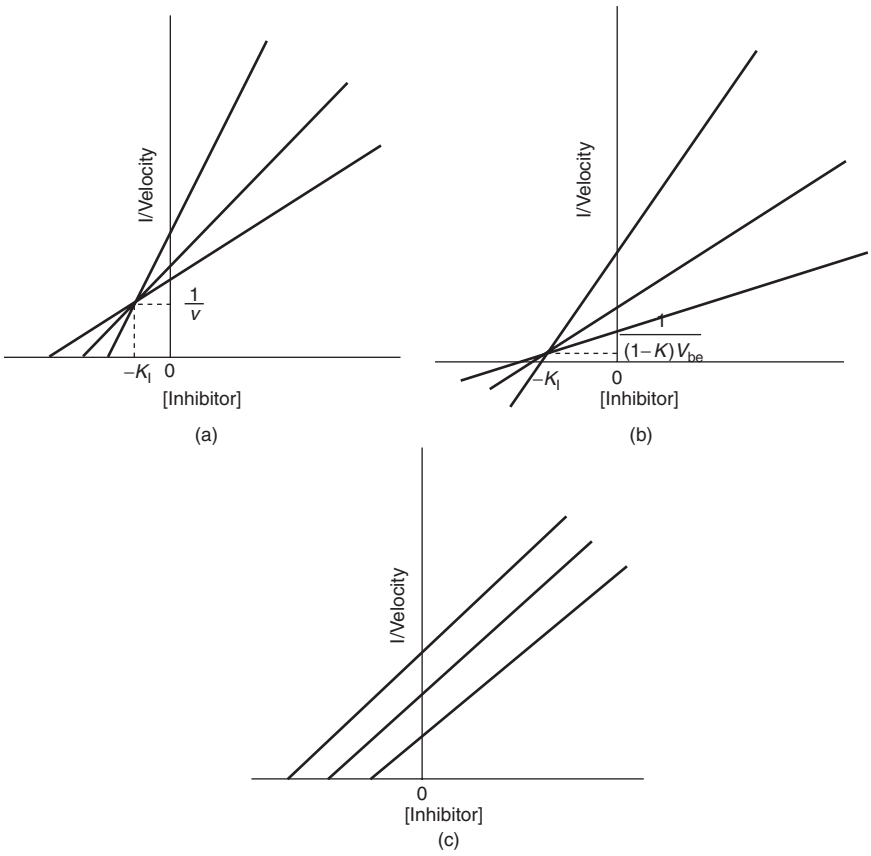

Figure 3.10 Dixon plots showing (a) competitive, (b) mixed, and (c) uncompetitive inhibition.

parameter is dependent on the concentrations of the substrate, inhibitor, and enzyme studied, whereas K_i values are independent of the substrate and thus more readily comparable across laboratories. IC_{50} plots are conventionally plotted as rate versus log [I], and the resulting curve can be described by Equation 3.22, where v_0 is the control rate, b is the background activity, S is the slope factor, and IC_{50} is the inhibitor concentration that reduces the velocity by 50%.

$$v = \frac{v_0}{1 + \left[\frac{[I]}{IC_{50}}\right]^S} + b \tag{3.22}$$

As with K_i determinations, the IC_{50} value should always be calculated using nonlinear regression of the untransformed data.

Owing to the complexity and time-consuming nature of K_i determinations, it is often favorable in drug discovery and development to determine IC_{50} values. The relationship between the K_i and the IC_{50} of an enzymatic reaction is influenced by the type of inhibition (Table 3.1). For example, with competitive and uncompetitive inhibitions, if the IC_{50} determination is made at $[S] \approx K_m$, then $K_i \approx \frac{1}{2}IC_{50}$, whereas for noncompetitive and mixed inhibitions, the IC_{50} and K_i values will be equal [41].

TABLE 3.1 Effects of Various Types of Reversible Inhibition on Kinetic Parameters and the Relationship Between K_i and IC_{50}

Type of Inhibition	Change in Kinetic Parameter by Inhibition			Relationship Between K_i and IC_{50} Values	
	V_{max}^{app}	K_m^{app}	V_{max}^{app}/K_m^{app}	General Equation	If [S] $\approx K_m$
Competitive	$\leftrightarrow$	$\uparrow$	$\downarrow$	$IC_{50} = K_i\left(1 + \frac{[S]}{K_m}\right)$	$\frac{1}{2}K_i = \frac{1}{2}IC_{50}$
Noncompetitive	$\downarrow$	$\leftrightarrow$	$\downarrow$	$IC_{50} = K_i$	$K_i = IC_{50}$
Uncompetitive	$\downarrow$	$\downarrow$	$\leftrightarrow$	$IC_{50} = K_i'\left(1 + \frac{K_m}{[S]}\right)$	$\frac{1}{2}K_i = \frac{1}{2}IC_{50}$
Mixed	$\downarrow$	$\uparrow$	$\leftrightarrow$	$IC_{50} = K_i'\left(\frac{K_m+[S]}{K_m'+[S]}\right)$	$K_i = IC_{50}$

3.6 CONCLUSIONS/FUTURE PERSPECTIVES

The determination of enzyme kinetics for drug metabolism reactions is an integral part of drug discovery and development. When carried out carefully and under the proper conditions, one can use these *in vitro* kinetic parameters in making predictions of a drug's potential *in vivo* pharmacokinetics and thus the "druggability" of the compound. Although most compounds follow hyperbolic, saturable (i.e., Michaelis–Menten) kinetics, one can also observe atypical kinetic profiles such as sigmoidal (autoactivation), biphasic, and substrate inhibition kinetics. Thus, it is critical to apply the correct kinetic model to enzyme kinetics data analyses to avoid making inaccurate conclusions about a compound's kinetics. *In vitro* determinations of a drug's potential for drug–drug interactions due to enzyme inhibition are also critical in assessing the potential *in vivo* utility of a compound. Again, one must assure use of the proper kinetic model when assessing propensity to inhibit drug-metabolizing enzymes.

As increasing numbers of compounds are being assessed for their metabolism characteristics during the discovery and development phase, one must continually look to more efficient methods for carrying out these analyses. For example, many high throughput technologies have been applied to ADME (absorption, distribution, metabolism, and excretion) studies such as 96-well-plate automation, parallel LC–MS methods, automated data processing, and sample pooling strategies [42]. Lastly, work will continue toward refining the *in vitro–in vivo* correlation models in an effort to better predict human *in vivo* metabolism from *in vitro* data. As we learn more about additional *in vivo* factors that control a drug's rate of metabolism *in vivo* and about intersubject variability in metabolism, these factors can be incorporated into models with the hope of improved predictions.

REFERENCES

1. Bjornsson T, Callaghan J, Einolf H *et al*. The conduct of *in vitro* and *in vivo* drug-drug interaction studies. Drug Metab Dispos 2003;31:815–832.
2. Tucker G, Houston J, Huang S. Optimizing drug development: strategies to assess drug metabolism/transporter interaction potential. Br J Clin Pharmacol 2001;52:107–117.

3. Yao C, Levy R. Inhibition-based metabolic drug-drug interactions: predictions from *in vitro* data. J Pharm Sci 2002;91:1923–1935.
4. Hermann M, Kase E, Molden E *et al*. Evaluation of microsomal incubation conditions on CYP3A4-mediated metabolism of cycosporin A by a statistical experimental design. Curr Drug Metab 2006;7:265–271.
5. Hutzler J, Wienkers L, Wahlstrom J *et al*. Activation of cytochrome P450 2 C9-mediated metabolism: mechanistic evidence in support of kinetic observations. Arch Biochem Biophys 2003;410:16–24.
6. Yamazaki H, Ueng Y, Shimada T *et al*. Roles of divalent metal ions in oxidations catalyzed by recombinant cytochrome P450 3A4 and replacement of NADPH: cytochrome P450 reductase with other flavoproteins, ferredoxin, and oxygen surrogates. Biochemistry 1995;34:8380–8390.
7. Shet M, Fisher C, Holmans P *et al*. Human cytochrome P450 3A4-enzymatic properties of a purified recombinant fusion protein containing NADPH-P450 reductase. Proc Natl Acad Sci U S A 1993;90:11748–11752.
8. Busby W, Ackermann J, Crespi C. Effect of methanol, ethanol, dimethyl sulfoxide, and acetonitrile on *in vitro* activities of cDNA-expressed human cytochrome P450s. Drug Metab Dispos 1999;27:246–249.
9. Tang C, Shou M, Rodrigues A. Substrate-dependent effect of acetonitrile on human liver microsomal cyctochrome P450 2 C9 (CYP2C9) activity. Drug Metab Dispos 2000;28:567–572.
10. Vuppugalla R, Chang S, Zhang H *et al*. Effect of commonly used organic solvents on the kinetics of cytchrome P450 2B6- and 2 C8-dependent activity in human liver microsomes. Drug Metab Dispos 2007;35:1990–1995.
11. Easterbrook J, Lu C, Sakai Y *et al*. Effects of organic solvents on the activities of cytochrome P450 isoforms, UDP-dependent glucuronyltransferase, and phenol sulfotransferase in human hepatocytes. Drug Metab Dispos 2001;29:141–144.
12. Chauret N, Gauthier A, Nicoll-Griffith D. Effect of common organic solvents on *in vitro* cytochrome P450-mediated metabolic activities in human liver microsomes. Drug Metab Dispos 1998;26:1–4.
13. Hickman D, Wang J, Wang Y *et al*. Evaluation of the selectivity of *in vitro* probes and suitability of organic solvents for the measurement of human cytochrome P450 monooxygenase activities. Drug Metab Dispos 1998;26:207–215.
14. Cotreau-Bibbo M, von Moltke L, Greenblatt D *et al*. Influence of polyethylene glycol and acetone on the *in vitro* biotransformation of tamoxifen and alprazolam by human liver microsomes. J Pharm Sci 1996;85:1180–1185.
15. Palamanda J, Feng W, Lin C *et al*. Stimulation of tolbutamide hydroxylation by acetone and acetonitrile in human liver microsomes and in a cytochrome P450 2 C9 reconstituted system. Drug Metab Dispos 2000;28:38–43.
16. Margolis J, Obach S. Impact of nonspecific binding to microsomes and phospholipid in the inihibition of cytochrome P4502D6: implications for relating *in vitro* inhibition data to *in vivo* drug interactions. Drug Metab Dispos 2003;31:606–611.
17. Austin R, Barton P, Cockroft S. The influence of nonspecific microsomal binding on apparent intrinsic clearance, and its prediction from physiochemical properties. Drug Metab Dispos 2002;30:1497–1502.
18. McLure J, Miners J, Birkett D. Nonspecific binding of drugs to human liver microsomes. Br J Clin Pharm 2000;49:453–461.
19. Obach R. Prediction of human clearance of twenty-nine drugs from hepatic microsomal intrinsic clearance data: an examination of *in vitro* half-life approach and nonspecific binding to microsomes. Drug Metab Dispos 1999;27:1350–1359.
20. Venkatakrishnan K, von Moltke L, Obach R. Microsomal binding of amitriptyline: effect on estimation of enzyme kinetic parameters *in vitro*. J Pharmacol Exp Ther 2000;293:343–350.

21. Carlile D, Zomorodi K, Houston J. Scaling factors to relate drug metabolic clearance in hepatic microsomes, isolated hepatocytes, and the intact liver: studies with induced livers involving diazepam. Drug Metab Dispos 1997;25:903–911.
22. Stone A, Mackenzie P, Galetin A. Isoform selectivity and kinetics of morphine 3- and 6-glucuronidation by human UDP-glucuronosyltransferases: evidence for atypical glucuronidation kinetics by UGT2B7. Drug Metab Dispos 2003;31:1086–1089.
23. Uchaipichat V, Galetin A, Houston J *et al*. Kinetic modeling of the interactions between 4-methylumbelliferone, 1-naphthol and zidovudine glucuronidation by UDP-glucuronosyltransferase 2B7 (UGT2B7) provides evidence for multiple substrate binding and effector sites. Mol Pharmacol 2008;74:1152–1162.
24. Zhou J, Tracy T, Remmel R. Glucuronidation of dihydrotestosterone and tran-androsterone by recombinant UDP-glucuronosyltransferase (UGT) 1A4: evidence for multiple UGT1A4 aglycone binding sites. Drug Metab Dispos 2010;38:431–440.
25. Hutzler J, Tracy T. Atypical kinetic profiles in drug metabolism reactions. Drug Metab Dispos 2002;30:355–362.
26. Segal I. Enzyme kinetics: behavior and analysis of rapid equilibrium and steady-state enzyme systems. New York: Wiley and Sons, Inc; 1975.
27. Shou M, Mei Q, Ettore M, *et al*. Sigmoidal kinetic model for two co-operative substrate binding sites in a cytochrome P450 3A4 active site: an example of the metabolism of diazepam and its derivatives. Biochem J 1999;340:845–853.
28. Shou M. Kinetic analysis for multiple substrate interactions at the active site of cytochrome P450. Methods Enzymol 2002;357:261–276.
29. Korzekwa K, Krishnamachary N, Shou M, *et al*. P450 kinetics with two substrate models: evidence that multiple substrates can simultaneously bind to cytochrome P450 active sites. Biochemistry 1998;371:4137–4147.
30. Lin Y, Lu P, Tang C, *et al*. Substrate inhibition kinetics for cyctochrome P450 catalyzed reactions. Drug Metab Dispos 2001;4:368–374.
31. Leskovac V. Comprehensive enzyme kinetics. New York: Kluwer Academic/Plenum Publishers; 2003.
32. Correia M, Ortiz de Montellano P. Cytochrome P450: structure, mechanism, and biochemistry. New York: Kluwer Academic/Plenum Publishers; 2005
33. Silverman R. The potential use of mechanism-based enzyme inactivators in medicine. J Enzyme Inhib 1988;2:73–90.
34. Nomeir A, Palamanda J, Favreau L. Optimization in drug discovery: *in vitro* methods. New Jersey: Humana Press; 2004.
35. Yang J, Jamei M, Rowland-Yeo K, *et al*. Kinetic values for mechanism-based enzyme inhibition: assessing the bias introduced by the conventional experimental protocol. Eur J Pharm Sci 2005;26:334–340.
36. Kitz R, Wilson I. Esters of methanesulfonic acid as irreversible inhibitors of acetylcholinesterase. J Biol Chem 1962;237:3245–3249.
37. Grimm S, Einolf H, Hall S, *et al*. The conduct on *in vitro* studies to address time-dependent inhibition of drug metabolizing enzymes: a perspective of the pharmaceutical research and manufacturers of America P(PhRMA). Drug Metab Dispos 2009;37:1355–1370.
38. Obach R, Walsky R, Venkatakrishnan K. Mechanism-based inactivation of human cytochrome P450 enzymes and the prediction of drug-drug interactions. Drug Metab Dispos 2007;35:246–255.
39. McConn D, Zhao Z. Integrating *in vitro* kinetic data from compounds exhibiting induction, reversible inhibition and mechanism-based inhibition: *in vitro* study design. Curr Drug Metab 2004;5:141–146.
40. Geng W. A method for identification of inhibition mechanism and estimation of Ki in *in vitro* enzyme inhibition study. Drug Metab Dispos 2003;31:1456–1457.

41. Cer R, Mudunuri U, Stephens R, *et al*. IC_{50}-to-K_i: a web-based tool for converting IC_{50} to K_i values for inhibitors of enzyme activity and ligand binding. Nucleic Acids Res 2009;37:441–445.
42. Kassel D. Applications of high-throughput ADME in drug discovery. Curr Opin Chem Biol 2004;8:339–345.